Acta Geochim (2016) 35(3):227–239
DOI 10.1007/s11631-016-0109-3

ORIGINAL ARTICLE

Nuclear field shift effects on stable isotope fractionation: a review

Sha Yang[1,2] · **Yun Liu**[1]

Received: 30 March 2016 / Revised: 9 May 2016 / Accepted: 12 May 2016 / Published online: 15 June 2016

Abstract An anomalous isotope effect exists in many heavy element isotope systems (e.g., Sr, Gd, Zn, U). This effect used to be called the "odd–even isotope effect" because the odd mass number isotopes behave differently from the even mass number isotopes. This mass-independent isotope fractionation driving force, which originates from the difference in the ground-state electronic energies caused by differences in nuclear size and shape, is currently denoted as the nuclear field shift effect (NFSE). It is found that the NFSE can drive isotope fractionation of some heavy elements (e.g., Hg, Tl, U) to an astonishing degree, far more than the magnitude caused by the conventional mass-dependent effect (MDE). For light elements, the MDE is the dominant factor in isotope fractionation, while the NFSE is neglectable. Furthermore, the MDE and the NFSE both decrease as temperatures increase, though at different rates. The MDE decreases rapidly with a factor of $1/T^2$, while the NFSE decreases slowly with a factor of $1/T$. As a result, even at high temperatures, the NFSE is still significant for many heavy element isotope systems. In this review paper, we begin with an introduction of the basic concept of the NSFE, including its history and recent progress, and follow with the potential implications of the inclusion of the NFSE into the kinetic isotope fractionation effect (KIE) and heavy isotope geochronology.

✉ Yun Liu
liuyun@vip.gyig.ac.cn

[1] State Key Laboratory of Ore Deposit Geochemistry, Institute of Geochemistry, Chinese Academy of Sciences, Guiyang 550081, China

[2] University of Chinese Academy of Sciences, Beijing 100049, China

Keywords Isotope fractionation · Mass-dependent effect · Nuclear field shift effect · Mass-independent fractionation · Nuclear volume effect · Nuclear shape effect

1 Introduction

From a spectroscopic view, isotope shifts include the mass shift and the field shift (King 1984). The mass shift is induced by the difference between isotope masses which is also called mass-dependent effect. The conventional equilibrium stable isotope fractionation theory for the mass shift was established by Bigeleisen and Mayer (1947) and by Urey (1947). This theory predicts that the isotope enrichment factor is proportional to the isotopic mass difference, Δm, and inversely proportional to the product of masses m and m′ of the two isotopes, when the temperature is constant. The field shift is a short expression of the nuclear field shift effect (NFSE), an anomalous isotope effect (i.e., mass-independent fractionation) caused by the difference in the nuclear size and shape of isotopes. It is also called the nuclear volume effect (NVE) because the nuclear shape effect is very small and the nuclear volume effect dominates. The nuclear field shift effect predominantly affects the isotope fractionation of heavy elements, but not light elements.

The anomalous isotope effect was first reported for metals by Fujii et al. (1989a, b) in the U(IV)–U(VI) exchange reaction. It is found that the isotope fractionation of the odd mass number isotope ^{235}U deviates from the mass-dependent lines defined by even mass number isotopes. The isotope fractionations of ^{157}Gd and ^{67}Zn are similar to ^{235}U which belong to mass-independent in liquid–liquid extraction experiments (Chen et al. 1992; Nishizawa et al. 1993). This anomalous isotope

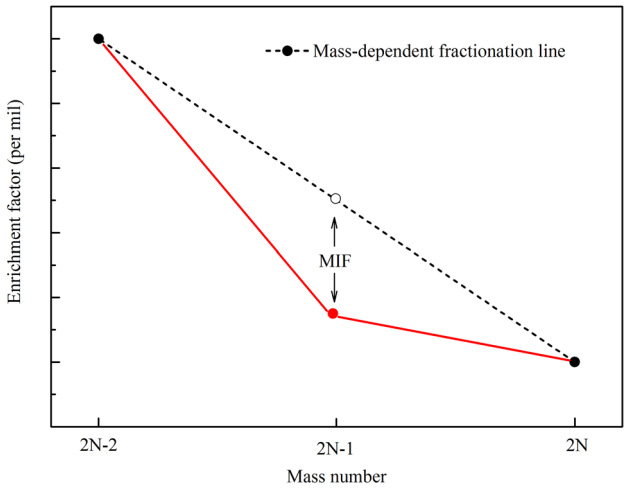

Fig. 1 Variation of the enrichment factor with isotopes. N is a positive integer. The *red line* is the real fractionation line. The *red solid circle* (the odd number isotope) deviates from the mass-dependent line composed of even mass number isotopes

fractionation phenomenon used to be called the "odd–even isotope effect" (Nishizawa et al. 1994) (Fig. 1) but its mechanism was not clear.

Nishizawa et al. (1995) interpreted the similar anomalous isotope effect of ^{87}Sr as being caused by the field shift in the liquid–liquid extraction of strontium chloride, using a crown ether. This is the first paper that clarified the cause of this kind of anomalous isotope effect. Nomura et al. (1996) found that ^{233}U shows anomalous mass-independent fractionations in the U(IV)–U(VI) exchange reaction, similar to those results in previous paper (Fujii et al. 1989a, b), and suggested that the cause was the field shift.

After a private communication with the Yasuhiko Fujii's group, Bigeleisen (1996) theoretically revised the reduced partition function ratios of uranium ions in solution. In his revision, the terms of the hyperfine splitting and the nuclear field shift effect (NFSE) were added to his theoretical treatment of isotope fractionation. He noticed that the hyperfine splitting was an order of magnitude smaller, explaining the anomaly in the ^{238}U/^{235}U separation in the U(III)–U(VI) exchange reaction. His results of the nuclear field shift effect are three times as large as the conventional mass-dependent fractionation, and show that heavier isotopes preferred to be enriched in U(IV) in the U(IV)–U(VI) exchange reactions. Since then, the NFSE has become an important correction term to the conventional Bigeleisen–Mayer equation for heavy elements. In a following paper, Bigeleisen also noticed that the NFSE was just a second order correction in chemical bonds (Bigeleisen 1998), indicating that the NFSE has a minor effect on vibrational frequencies (i.e., on the conventional mass-dependent isotope fractionation). Importantly, the paper first pointed out that the NFSE could induce large isotopic fractionations through the variation of ground-state electronic energy alone.

The nuclear field shift effect scales with the difference in the mean-square nuclear charge radius of different isotopic nuclei (i.e., NFSE $\propto \delta\langle r^2\rangle$ and $\delta\langle r^2\rangle = \langle r^2\rangle_A - \langle r^2\rangle_{A'}$, where A and A′ represent heavy and light isotopes, respectively) (King 1984). A well-known phenomenon is that the mean-square nuclear radii (i.e., $\langle r^2\rangle$) do not follow a simple straight line with the number of neutrons increasing. Odd atomic mass number isotopes of many heavy elements (e.g., ^{235}U) tend to be smaller than the trend line through the adjacent isotopes with even atomic mass numbers (e.g., ^{234}U and ^{236}U) of the same element. This is called odd–even staggering in the atomic spectra (King 1984) (Fig. 2a). The above-

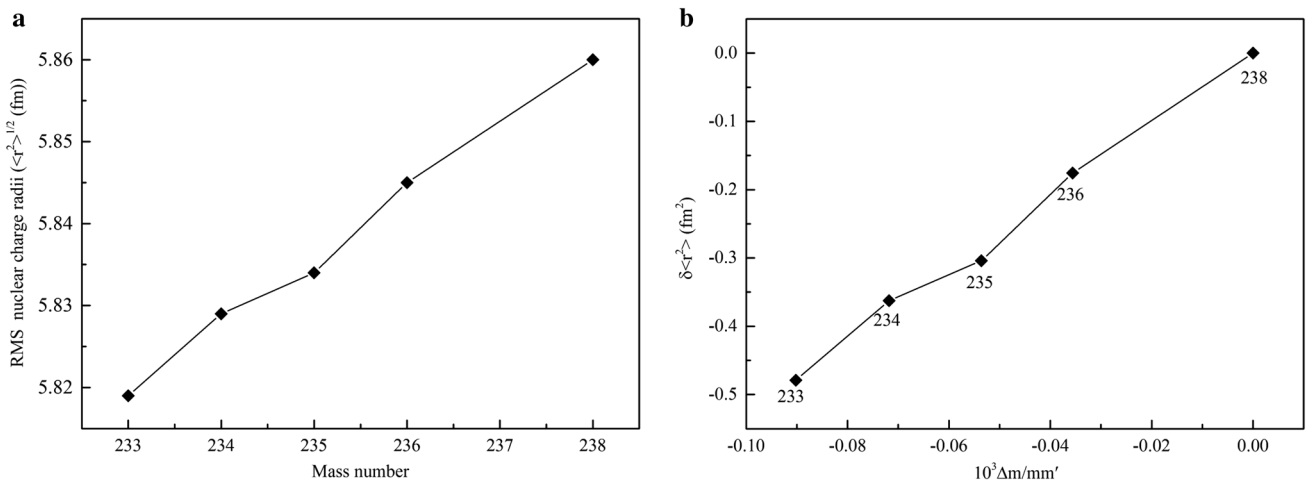

Fig. 2 **a** Root mean-square (RMS) nuclear charge radii ($\langle r^2\rangle^{1/2}$) of U isotopes (Fricke and Heilig 2004). The odd atomic mass number isotope (^{235}U) is smaller than the trend line through the even atomic mass number isotopes (^{234}U and ^{236}U). **b** Plots of $\delta\langle r^2\rangle$ vs. $\Delta m/mm'$ for U isotopes, showing not a *straight line*

mentioned odd–even isotope effect is similar to the odd–even staggering. Moreover, $\delta < r^2 >$ varies with $\Delta m/mm'$ nonlinearly, which shows that the nuclear field shift effect induces mass-independent isotope fractionation (Fig. 2b).

The experiments also find the heavier isotopes of U to be preferentially enriched in U(IV) rather than U(VI) in redox reactions (Fujii et al. 1989a; Nomura et al. 1996, Wang et al. 2015). However, the conventional isotope fractionation theory estimates that the heavier isotopes (^{54}Cr, ^{56}Fe, ^{238}U, etc.) would be enriched in the higher oxidized states instead of the lower oxidized states. Assumedly, such mismatch is caused by the NFSE, but with no further evidence. This could be an important research topic for the near future.

2 Conventional mass-dependent fractionation

2.1 Isotope fractionation factor α

Consider an isotope exchange reaction

$$A'Y + AX = A'X + AY \quad (1)$$

where A and A′ are the heavy and light isotopes of the element A; X and Y are different compounds. The isotope fractionation factor for this reaction is defined as $\alpha = (A/A')_{AY}/(A/A')_{AX}$, an isotope concentration ratio between AX and AY. The isotope enrichment factor is defined as $\varepsilon = \alpha - 1 \approx \ln\alpha$.

2.2 Bigeleisen–Mayer theory or Urey model

Bigeleisen and Mayer (1947) and Urey (1947) proposed a well-known equation for calculating the isotope fractionation extent of an isotope exchange reaction, called the Bigeleisen–Mayer equation (hereafter the B–M equation) or the Urey model. This equation, actually based on the Born–Oppenheimer approximation, assumes several harmonic approximations as well. According to the B–M equation, the logarithm of the isotope fractionation factor for the exchange reaction (1) is

$$\ln\alpha_0 = \ln(s/s')f(AY/A'Y) - \ln(s/s')(AX/A'X) \quad (2)$$

where (s/s′)f is the reduced partition function ratio (RPFR).

Under high-temperature approximations, the (s/s′)f of AX/A′X is

$$(s/s')f(AX/A'X) = 1 + \Delta m m_x n_x u_x^2/24\, mm' \quad (3)$$

where m and m′ are the masses of the heavy and light isotopes, respectively; Δm is the relative mass difference of isotopes (i.e., $\Delta m = m - m'$); m_x is the mass of the compound X; and n_x is the number of compound X. In Eq. (3), u_X is defined as

$$u_X = (hc/kT)\omega_X \quad (4)$$

where h and k are Planck and Boltzmann constants; c is light velocity; T is the absolute temperature and ω_X is the wave number of the harmonic oscillation of the stretching motion. The expression of (s/s′)f(AY/A′Y) is similar to(s/s′)f(AX/A′X). So the expression of the isotope enrichment factor is

$$\varepsilon \approx \ln\alpha_0 = (hc/kT)^2\left(m_Y n_Y \omega_Y^2 - m_X n_X \omega_X^2\right)\Delta m/24 mm' \quad (5)$$

From Eq. (5), the enrichment factor is proportional to $\Delta m/(mm'T^2)$. When the temperature is constant, the enrichment factor is proportional to $\Delta m/mm'$. Therefore, the isotope fractionation factor decreases with the increasing atomic number. According to the B-M equation, the isotope fractionation of heavy elements would be extremely small even at low temperatures.

The mass-dependent fractionation (MDF), as described by the B-M equation, only considers the difference in kinetic energies (i.e., rotational energy, translational energy, and vibrational energy) of the two isotopologues, neglecting the difference in their electronic energies. This approximation treatment is, however, improper for heavy elements. The MDF contribution is only one part of the total isotope fractionation.

2.3 Revised isotope fractionation theory

For a uranium isotope exchange reaction, Fujii and coworkers (1989a) found the ratio of theoretically predicted isotope enrichment factors between ^{234}U/^{235}U and ^{235}U/^{238}U is 1/3. This is distinctly different from the experimental value of 1/7. In addition, they observed a clear deviation from the mass-dependent isotope fractionation line theoretically predicted by the B-M equation for ^{235}U.

Bigeleisen (1996) extended the isotope fractionation factor containing the nuclear spin and the nuclear field shift effect as well as the mass-dependent effect. The logarithm of the revised isotope fractionation factor becomes (Bigeleisen 1996)

$$\varepsilon \approx \ln\alpha = \ln\alpha_0 + \ln K_{anh} + \ln K_{BOELE} + \ln K_{fs} + \ln K_{hf} \quad (6)$$

where $\ln\alpha_0$ is the isotope fractionation factor under the B-M equation approximations; $\ln K_{anh}$ is the anharmonic correction term; $\ln K_{BOELE}$ is the correction to the Born–Oppenheimer approximation; $\ln K_{fs}$ is the contribution from the nuclear field shift effect; and $\ln K_{hf}$ is the term for nuclear spin effect. Because of extremely small contributions of the anharmonic correction for heavy elements, the $\ln K_{anh}$ can be neglected (Bigeleisen 1996) in calculating

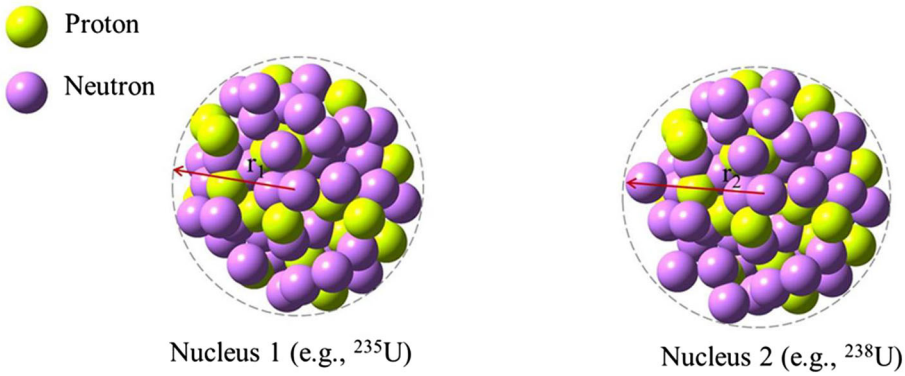

Fig. 3 Nuclei of the isotopes of heavy elements with finite nuclear sizes. The different numbers of neutrons cause the difference in nuclear size and shape of isotopes (i.e., difference in nuclear radius r_1 and r_2). For example, the root mean-square nuclear charge radius $<r^2>^{1/2}$ of ^{235}U and ^{238}U are 5.834 fm and 5.860 fm (Fricke and Heilig 2004), respectively

the enrichment factor for heavy elements. The correction to Born–Oppenheimer approximation is related to masses of isotopes and is proportional to $\Delta m/mm'$ (Kleinman and Wolfsberg 1973, 1974). Therefore, $\ln\alpha_0$ and $\ln K_{BOELE}$ are both proportional to $\Delta m/mm'$ when the temperature is constant. Nuclear spin effect exists only when the isotopic mass number is odd. Bigeleisen (1996) indicates that the nuclear spin effect is too small to account for the anomalous isotope effect of $^{238}U/^{235}U$ separation in the U(III) and U(VI) exchange reaction and can be safely neglected in the investigation of U isotope exchange reactions.

Under the approximations used in the B–M equation, a nucleus is considered as a point charge. However, the isotopes of heavy elements have the same number of protons but different number of neutrons. This can cause the difference in nuclear size and shape (e.g., ^{235}U vs. ^{238}U) (Fig. 3). Therefore, their ground-state electronic energies will also be different (Table 1). The difference in electronic energies can no longer be neglected for the isotopes of heavy elements. This is completely ignored in the conventional B–M equation.

3 Nuclear field shift effect

In the 20th century, several researchers (e.g., Stacey 1966; Heilig and Steudel 1978; King 1984; Aufmuth et al. 1987) proposed the concept of the "nuclear field shift effect" in the atomic spectra but failed to apply it to the study of isotope fractionation. The nuclear field shift effect is related to the difference in ground-state electronic energies caused by the difference in nuclear size and shape. For the isotope exchange reaction Eq. (1), the NFSE (i.e., $\ln K_{fs}$) is written as (e.g., Bigeleisen 1996)

$$\ln K_{fs} = (kT)^{-1}\{[E^0(AX) - E^0(A'X)] - [E^0(AY) - E^0(A'Y)]\} \quad (7)$$

where E^0 is the ground-state electronic energy; AX and A′X represent compounds with different isotopes. Equation (7) shows that the NFSE value is proportional to 1/T, while the MDE scales with $1/T^2$ (Eq. (5)). If the temperature is at constant, the values of the NFSE will be proportional to the difference in ground-state electronic energies caused by isotope substitutions.

The effect of nuclear field shift is also considered to be proportional to the electron density at the nucleus (King 1984). The electron density at the nucleus is expressed as $|\Psi(0)|^2$ (also called contact density):

$$\delta E_{fs} \propto \left(|\Psi(0)_A|^2 - |\Psi(0)_B|^2\right) \times \delta <r^2>_{ij} \quad (8)$$

where δE_{fs} is the difference in NFSE-driven ground-state energies; $\delta <r^2>$ is the difference in mean-square nuclear charge radii of the two isotopic nuclei; i and j represent the heavy and light isotopes.

4 Mass-independent fractionation (MIF)

Mass-independent fractionation refers to the deviation from the mass-dependent isotope fractionation line. Taking Hg isotopes as an example, the $\delta^i Hg$ is defined as

$$\delta^i Hg = \left[\left(^iHg/^{198}Hg\right)_{sample}/\left(^iHg/^{198}Hg\right)_{ref} - 1\right] \times 1000 \quad (9)$$

and the MIF of any pair of Hg isotopes (e.g., $^iHg/^{198}Hg$) becomes

$$\Delta^i Hg = \delta'^i Hg - \lambda_{MD}\delta'^{202}Hg \quad (10)$$

where $\delta'^{202}Hg = 1000 \times \ln\left(1 + \frac{\delta^{202}Hg}{1000}\right)$ (Miller 2002; Young et al. 2002), and λ_{MD} is the conventional mass-dependent scaling factor.

Unfortunately, the $\Delta^i Hg$ values cannot be obtained through theoretical methods because the values of $\delta^{202}Hg$

Table 1 Calculated total energies (i.e., electron energies plus nuclear repulsion energies) of mercury atoms, ions, and molecules

	E(^{202}Hg) (Hartree)	E(^{198}Hg) (Hartree)	ΔE (^{202}Hg–^{198}Hg) (Hartree)
Hg^0	−19648.872900452	−19648.899279761	0.026379309
Hg^{2+}	−19647.928339749	−19647.954715647	0.026375898
$HgCl_2$	−20570.839876388	−20570.866254331	0.026377943
$HgBr_2$	−24858.786154305	−24858.812532295	0.026377990
$Hg(CH_3)Cl$	−20149.473020068	−20149.499398518	0.026378450
$Hg(CH_3)_2$	−19728.085945293	−19728.112323991	0.026378698
$HgCl_3^-$	−21031.911516436	−21031.937893728	0.026377292
$HgCl_4^{2-}$	−21492.847297638	−21492.873674561	0.026376923
$HgBr_3^-$	−27463.831015157	−27463.857392566	0.026377409
$HgBr_4^{2-}$	−30068.742826148	−30068.769203205	0.026377057
$Hg(H_2O)_6^{2+}$	−20104.905854632	−20104.932230959	0.026376327
$Hg(OH)_2$	−19799.820912939	−19799.847291190	0.026378251

These data are from Yang and Liu (2015). 1 Hartree = 627.51 kcal/mol

for a fractionation species cannot be calculated. Instead of the absolute value of $\Delta^i Hg$ for species A or B, the relative MIF of species A comparing with species B (i.e., $\Delta^i Hg_{A-B}$) can be calculated, thus:

$$\begin{aligned}\Delta^i Hg_A &= \left(\delta'^i Hg_B + \ln^i\alpha_{A-B}\right) \\ &\quad - \lambda_{MD}\left(\delta'^{202} Hg_B + \ln^{202}\alpha_{A-B}\right) \\ &= \Delta^i Hg_B + (\lambda - \lambda_{MD})\ln^{202}\alpha_{A-B} \end{aligned} \quad (11)$$

Therefore, the mass-independent fractionation between species A and B is

$$\Delta^i Hg_A - \Delta^i Hg_B = (\lambda - \lambda_{MD})\ln^{202}\alpha_{A-B} \quad (12)$$

$$\lambda = \frac{\ln^i\alpha_{A-B}}{\ln^{202}\alpha_{A-B}} \quad (13)$$

$$\begin{aligned}\ln^i\alpha_{A-B} &= \lambda_{NFS}\ln^{202}\alpha^{NFS}_{A-B} + \lambda_{MD}\ln^{202}\alpha^{MD}_{A-B} \\ &\quad + \lambda_{MIE}\ln^{202}\alpha^{MIE}_{A-B} + \lambda_{Other}\ln^{202}\alpha^{other}_{A-B}\end{aligned} \quad (14)$$

$$\begin{aligned}\ln^{202}\alpha_{A-B} &= \ln^{202}\alpha^{NFS}_{A-B} + \ln^{202}\alpha^{MD}_{A-B} + \ln^{202}\alpha^{MIE}_{A-B} \\ &\quad + \ln^{202}\alpha^{other}_{A-B}\end{aligned} \quad (15)$$

where λ_{NFS} is the nuclear field shift scaling factor; λ_{MIE} is the magnetic isotope effect scaling factor; λ_{Other} is any other scaling factors and $\ln\alpha^{other}$ is fractionation driven by other causes except the MDE, the NFSE and the MIE. Here if only the MIF caused by the NFSE is considered, it would be

$$\Delta^i_{NFS}Hg_A - \Delta^i_{NFS}Hg_B = (\lambda_{NFS} - \lambda_{MD})\ln^{202}\alpha^{NFS}_{A-B} \quad (16)$$

where λ_{MD} is calculated using the high temperature approximation of equilibrium fractionation (Young et al. 2002). Because the values of λ_{MD} are weakly temperature-dependent for heavy element isotope systems (Cao and Liu 2011), we have,

$$\lambda_{MD} = \frac{\left(\frac{1}{m_i} - \frac{1}{m_j}\right)}{\left(\frac{1}{m_i} - \frac{1}{m_k}\right)} \quad (17)$$

and λ_{NFS} is from the mean square nuclear charge radii (Schauble 2007):

$$\lambda_{NFS} = \frac{\langle r_i^2\rangle - \langle r_j^2\rangle}{\langle r_i^2\rangle - \langle r_k^2\rangle} \quad (18)$$

where m_i, m_j and m_k are the masses of isotopes i, j and k, respectively, and $\langle r_i^2\rangle$, $\langle r_j^2\rangle$ and $\langle r_k^2\rangle$ are their mean square nuclear charge radii.

Other equations for calculating the MIF caused by the NFSE were proposed by Ghosh et al. (2008) (i.e., $\Delta^i Hg = (A^i_{NV} - A^i_{MD})\delta^{198}Hg$) and Yang and Liu (2015) (i.e., $\Delta^A_{NV}Hg = (\lambda_{NV} - \lambda_{MD})\delta'^{202}Hg$) for experiments, where A^i_{NV} and λ_{NV} are nuclear field shift scaling factors that are equal to λ_{NFS}, and A^i_{MD} is mass-dependent scaling factors that are equal to λ_{MD}. These two equations are reasonable only when the value of δ is caused by the nuclear field shift effect (i.e., δ^{NFS}).

5 Experimental and theoretical studies for NFSE

5.1 Liquid–liquid extraction experiments

Fujii and his coworkers investigated the nuclear field shift effect of stable isotope equilibrium fractionation of various elements by liquid–liquid extraction experiments, including Ti, Zn, Zr, Fe, Gd, Nd, Cr, Sr, Mo, Ru, Te, Cd and Sn and other isotope systems (Fujii et al. 1998a, b;

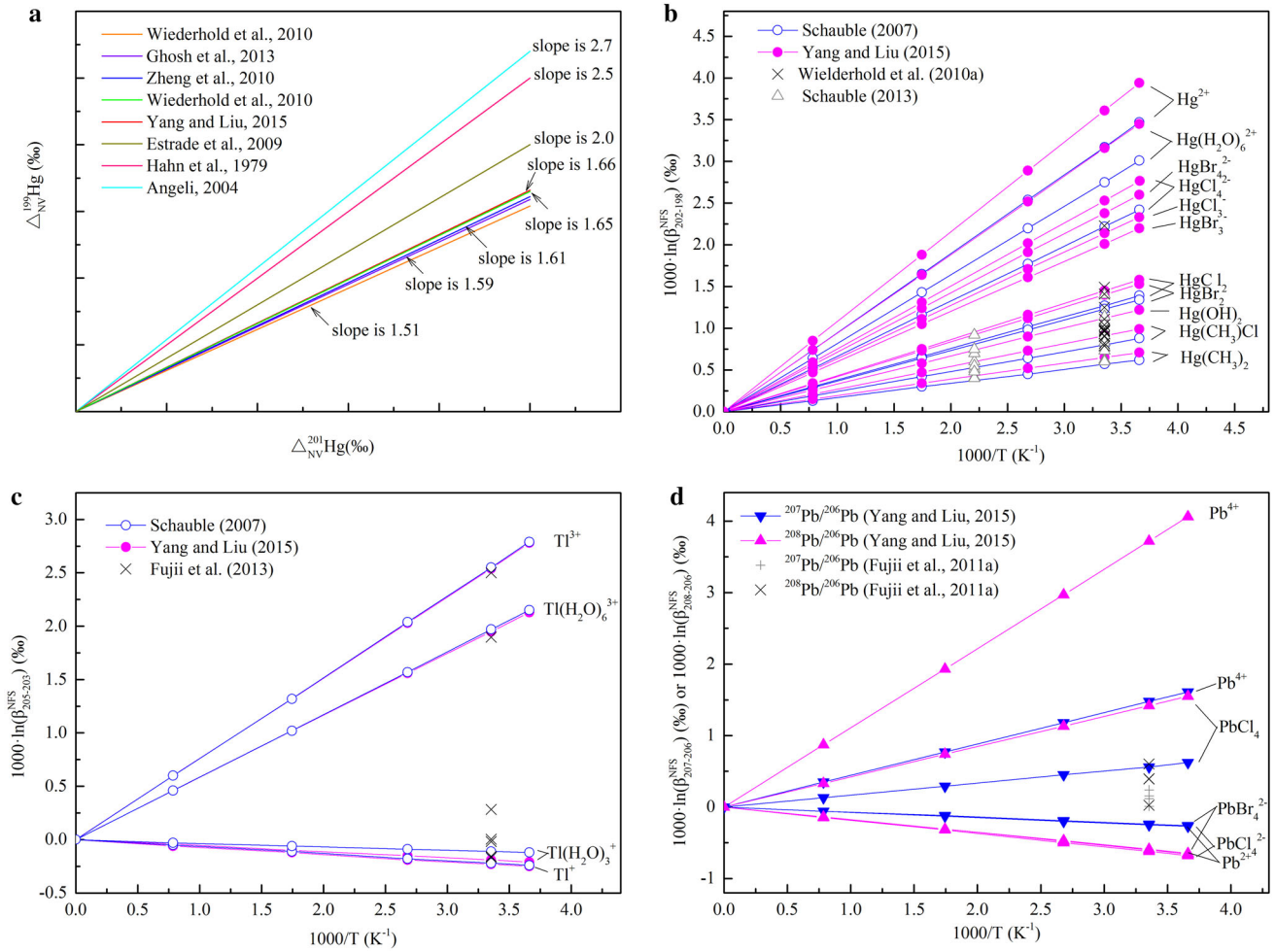

Fig. 4 The NFSE-driven fractionations of Hg, Tl, Pb and U systems. **a** Different slopes of 199-MIF vs. 201-MIF. **b** The NFSE-driven fractionations of Hg-bearing species relative to Hg^0. $HgCl_4^{2-} > HgCl^+ > HgOH^+ > HgCl_2 > HgClOH > HgSHCl > Hg(OH)_2 > Hg SMeCl > Hg(SH)^+ > HgSHOH > Hg(SH)_2 > HgSMeOH > Hg(Sme)_2 > Hg(Sme)^+$, at 25 °C (Wiederhold et al. 2010). Schauble (2013) calculate the NFSE in Hg crystals [$HgO_{(s)} > HgS_{(s)} > Hg_2Cl_{2(s)} > Hg_2Cl_{2(g)} > \beta$-Hg(s) > fcc-Hg(s) > α-Hg(s) > bcc-Hg(s) > sc-Hg(s)] at 25 and 180 °C. **c** The NFSEs-driven fractionations of Tl-bearing species relative to Tl^0. Fujii et al. (2013) only calculated the NFSEs at 25 °C [$Tl^{3+} > Tl(H_2O)^{3+} > TlO^- > TlCl > 0 > TlO^+ > Tl^+ > Tl(H_2O)^+ > TlCl^{2+}$]. **d** The NFSE-driven fractionations of the Pb-bearing species, relative to Pb^0 (Yang and Liu 2015), and Pb^{2+} (Fujii et al. 2011a, b). Fujii et al. (2011a) only estimates the NFSEs at 25 °C [$PbO > Pb^0 > PbCl + > Pb(H_2O)^{2+} > 0$]. **e** The NFSEs-driven fractionations of the U(III)–U(IV) system at MCDCHF level (Abe et al. 2008a), the DCHF method with the Gaussian-type finite-nucleus model using the three basis sets (dz–dz, tz-dz and tz-dz) (Abe et al. 2008b) and one experimental result (2.7) (Dujardin and Lonchampt 1992; Lerat and Lorrain 1985) at 293 K. **f** The NFSE-driven fractionations of the U(IV)–U(VI) system at 308 K. Abe et al. (2008b) calculates it using three basis sets, with and without the BSSE corrections, at the DCHF level with the Gaussian nucleus model (NFSE values: BSSE uncorrected dz–dz > BSSE corrected tz–tz > BSSE uncorrected tz–tz > BSSE corrected tz-dz > BSSE uncorrected tz-dz > BSSE corrected dz–dz). The results of Abe et al. (2010) show the NFSE results of U^{4+}– $UO_2Cl_3^- = U^{4+}$–$UO_2Cl_4^{2-} > UF_4$–$UO_2F_4^{2-} > UCl_4$–$UO_2Cl_3^- = UCl_4$–$UO_2Cl_4^{2-} > UBr_4$–$UO_2Br_4^2 > U^{4+}$–$UO_2^{2+} > 0 > UCl_4$–UO_2^{2+}. The corresponding experimental value is 2.24 (Fujii et al. 2006c)

Nishizawa et al. 1998; Fujii et al. 1999a, b, 2000, 2002; Shibahara et al. 2002a, b; Fujii et al. 2006a, b, 2008, 2009a, b, c; Moynier et al. 2009a, b; Fujii et al. 2010).

Equation (8) can be written specifically as follows in the atomic spectra (King 1984):

$$\delta T = \pi|\Psi(0)|^2 \frac{a_0^3}{z} f(z)\delta <r^2> \quad (19)$$

where f(z) is a known function of z; a_0 is Bohr radius and z is the atomic number. Therefore, the simplification of the Eq. (19) (Fujii et al. 1999a) is

$$\ln K_{fs} = b\delta <r^2> \quad (20)$$

where b is the scaling factor of the nuclear field shift effect.

When the temperature is constant, the $\ln\alpha_0 \propto \Delta m/mm'$ and $\ln K_{BOELE} \propto \Delta m/mm'$ can be obtained by the analysis of the second part. Since $\ln K_{anh}$ can be neglected, Eq. (6) can be simplified as follows:

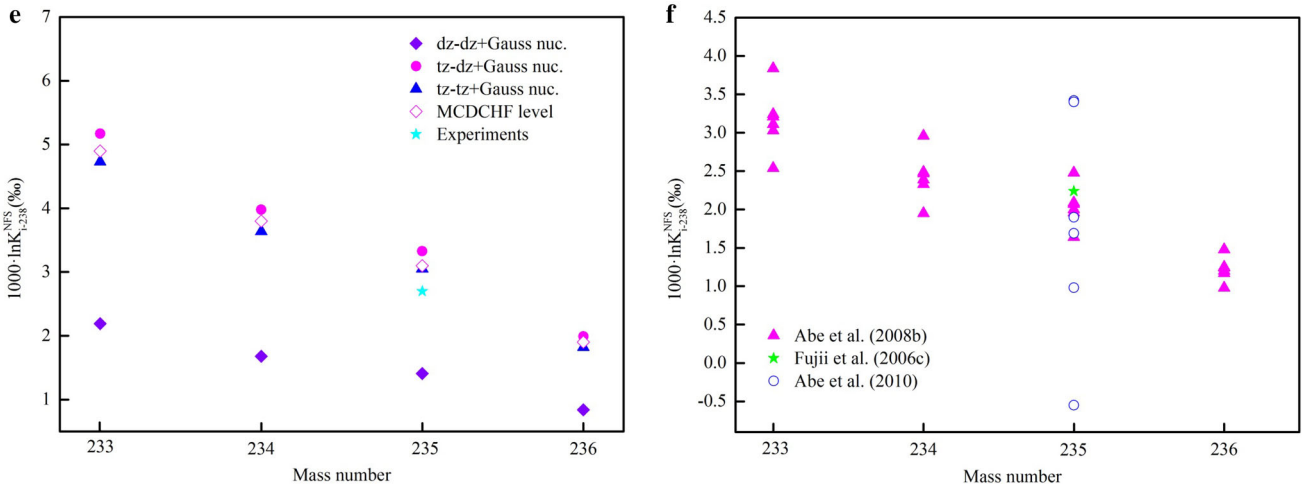

Fig. 4 continued

$$\varepsilon \approx \ln\alpha = a\frac{\Delta m'}{mm} + b\delta\langle r^2\rangle + \ln K_{hf} \quad (21)$$

where the first term is the conventional Bigeleisen–Mayer term; the second term is the nuclear field shift effect term; the third term is the nuclear spin term; a and b are scaling factors of these two terms. The isotope fractionation factor α can be obtained from experiments [i.e., $\alpha = (A/A')_{AY}/(A/A')_{AX}$]. The mean square of the charge distribution radii of the nuclei are available from previous studies (e.g., Fricke and Heilig 2004; Angeli 2004). Thus, Eq. (21) has three unknown parameters, a, b and $\ln K_{hf}$.

Fujii and coworkers used the isotope pairs to calculate the scaling factors and the nuclear spin effect. For example, for titanium isotopic equilibrium fractionation (Fujii et al. 1998a), they used three isotope pairs, ^{48}Ti–^{46}Ti, ^{48}Ti–^{47}Ti and ^{48}Ti–^{50}Ti. Thus, they got three equations,

$$\varepsilon_{48-46} = a(\Delta m/mm')_{48-46} + b\delta\langle r^2\rangle_{48-46} \quad (22)$$

$$\varepsilon_{48-47} = a(\Delta m/mm')_{48-47} + b\delta\langle r^2\rangle_{48-47} + (\ln K_{hf})_{48-47} \quad (23)$$

$$\varepsilon_{48-50} = a(\Delta m/mm')_{48-50} + b\delta\langle r^2\rangle_{48-50} \quad (24)$$

They obtained ε_{i-j} value from experiments and got the $\langle r^2\rangle_{i,j}$ value from the previous literatures, and calculated a, b and $\ln K_{hf}$ from the above three equations, where i and j represent isotopes 46, 47, 48 and 50.

5.2 Liquid–vapor evaporation experiments

There is another type of experiment of liquid–vapor evaporation for studying the nuclear field shift effect. Estrade et al. (2009) and Ghosh et al. (2013) conducted liquid–vapor evaporation experiments in the absence of light for mercury. They both concluded that the nuclear field shift effects are the dominant cause of equilibrium stable isotope fractionation in the absence of light. In addition, experiments were conducted to estimate the mass-independent fractionation of Hg isotopes during abiotic reduction (Bergquist and Blum 2007; Zheng and Hintelmann 2010a) and photoreduction in natural water (Zheng and Hintelmann 2009). They observed that ^{199}Hg and ^{201}Hg are enriched in the reactant Hg(II) due to the MIF caused by photo-reduction, while the product Hg^0 enrich ^{199}Hg and ^{201}Hg where the MIF observed in the absence of light. Zheng and Hintelmann (2010b) also investigated the isotope fractionation of mercury during photochemical reduction by low-molecular-weight organic compounds. They observed the nuclear shift effect in the photochemical reduction by serine.

Estrade et al. (2009) found that MIFs for odd isotopes (^{199}Hg and ^{201}Hg) and small MIFs for even isotope (^{200}Hg) in the vapor phase (Hg^0) are caused by the NFSE in the temperature range of 2–22 °C. Their average results of Δ^{199}_{NFS}Hg, Δ^{201}_{NFS}Hg and Δ^{200}_{NFS}Hg values are 0.1 2 ‰, 0.07 ‰ and 0.01 ‰ for Hg^0, respectively. The results of equilibrium evaporation experiments of Ghosh et al. (2013) are similar to those of Estrad et al. (2009) and their average Δ^{199}_{NFS}Hg, Δ^{201}_{NFS}Hg and Δ^{200}_{NFS}Hg values for Hg^0 are 0.14 ‰ ± 0.01 ‰, 0.09 ‰ ± 0.01 ‰ and 0.01 ‰ ± 0.03 ‰, respectively. Taking the error into account, there is almost no mass-independent fractionation for the even isotope (^{200}Hg).

Wiederhold et al. (2010) also investigated the mercury mass-independent fractionations experimentally and theoretically. It is found that the Δ^{199}_{NFS}Hg scales with Δ^{201}_{NFS}Hg in a slope of 1.51 (Wiederhold et al. 2010), 1.59 (Ghosh et al. 2013), 1.61 (Zheng and Hintelmann 2010a), and 2.0 (Estrade et al. 2009) (Fig. 4a). Moynier et al. (2013) reviewed the

isotopic variations (e.g., U and Tl) caused by the nuclear field shift effect in different natural environments, such as in meteorites and at low- or high-temperatures.

5.3 Theoretical calculations of NFSE

5.3.1 NFSE in gaseous and small liquid species

Schauble (2007) is the first to perform quantum chemistry calculations of the equilibrium isotope fractionation factors with the consideration of the NFSE. He studied mercury- and thallium-bearing species with the revision of the Bigeleisen–Mayer equation, including the mass-dependent isotope fractionation and the nuclear field shift isotope fractionation. He directly calculated the ground-state electronic energies of isotopic substitution through the Gaussian exponent ξ ($\xi = 3/2 <r^2>$) using the mean square nuclear charger radii of Angeli (2004) by the Dirac 04 software package and obtained the values of the NFSE by Eq. (7).

Schauble (2007) optimized the molecular geometries at a pseudo-potential HF level by using Gaussian 03. Then he used the optimized geometry results as initial guesses for the second run of optimization in Dirac 04. He used the all-electron Dirac–Hartree–Fock theory to calculate the relativistic electron structures through the iteratively quadratic fitting method, i.e., to optimize the structures to their lowest energy points by adjusting the bond length stepwise, because the species in his study are all in high symmetry. His calculations indicated that the isotopic variation in the nuclear field shift is the dominant cause of equilibrium fractionation, driving $^{205}Tl/^{203}Tl$ and $^{202}Hg/^{198}Hg$ fractionations up to 3 ‰ at room temperature. But mass-dependent fractionations are much smaller than the NFSE, only ca. 0.5 ‰–1 ‰ for the same isotopes.

So far, there have been only a few NFSE-included fractionation factors that are determined by theoretical calculations, such as those for uranium, lead, mercury and thallium isotopes (Abe et al. 2008a, b, 2010; Fujii et al. 2011a; Schauble 2007; Wiederhold et al. 2010; Ghosh et al. 2013; Fujii et al. 2013; Yang and Liu 2015) (Fig. 4b–f). These authors all found that the nuclear field shift effect was the dominant controlling factor for isotope fractionation of the heavy elements, far more important than the conventional mass-dependent effects. Anomalous light isotope enrichments of U(IV), U(VI), Pb(II) and Tl(I) relative to U(III), U(IV), Pb^0 and Tl^0 were found (Schauble 2007; Abe et al. 2008a, b, 2010; Fujii et al. 2011a, 2013; Yang and Liu 2015). In addition, zinc (Fujii et al. 2009c, 2010) and nickel isotopes (Fujii et al. 2011b) were studied both experimentally and theoretically. However, the NFSE was found to be much smaller than the conventional mass-dependent effects for their cases.

The calculation of Schauble (2007), Wiederhold et al. (2010), Ghosh et al. (2013) and Yang and Liu (2015) all showed that a part of the MIFs of Hg-bearing species are caused by the nuclear field shift effect. These authors found that the NFSE-driven MIFs of odd mass number isotopes ($\Delta^{199}_{NFS}Hg$ and $\Delta^{201}_{NFS}Hg$) are larger than that of the even mass number isotope ($\Delta^{202}_{NFS}Hg$). Plotting the $\Delta^{199}_{NFS}Hg$ against $\Delta^{201}_{NFS}Hg$, all the data fall into a straight line with the slope of 1.65 (Wiederhold et al. 2010), or 1.66 (Yang and Liu 2015) if using the nuclear charge radii of Fricke and Heilig (2004). It agreed well with the experimental results. However, the results would deviate far away from the experimental slopes when other nuclear charge radii are used, such as the slope of 2.7 [$< r^2 >$ values are from Angeli (2004)], and 2.5 ($< r^2 >$ from Hahn et al. 1979) (Fig. 4a), showing the nuclear charge radii from Fricke and Heilig (2004) are more reasonable for the Hg-NFSE theoretical investigation. The slope of $\Delta^{199}_{NFS}Hg$ / $\Delta^{201}_{NFS}Hg$ only relates to the conventional mass-dependent scaling factor (i.e., λ_{MD}) and the nuclear field shift scaling factor (i.e., λ_{NFS}). It is independent of the absolute values of $\Delta^{199}_{NFS}Hg$ and $\Delta^{201}_{NFS}Hg$, and the variation in temperature. Therefore, the slope will be a constant value of 1.64 (without rounding off the numbers) when the radii of the Landolt–Boernstein Database (Fricke and Heilig 2004) are used as the temperature varies from 0 °C to 1000 °C or even higher.

The results of ^{200}Hg-MIF caused by the NFSE of Yang and Liu (2015) exclude the nuclear field shift from the causes of large ^{200}Hg-MIF found in the field observations of Gratz et al. (2010) and Chen et al. (2012). The results of snow sample from subarctic zone are much larger and in opposite directions (Chen et al. 2012). Therefore, there must be other mechanisms to produce such large ^{200}Hg-MIF signals instead of the NFSE. Yang and Liu (2015) also investigates the NFSE-driven MIFs of Pb-bearing species. They found that the magnitudes of odd mass number MIF ($\Delta^{207}_{NFS}Pb$) are almost equal to those of even mass number MIF ($\Delta^{204}_{NFS}Pb$) but in opposite directions (i.e., $\Delta^{207}_{NFS}Pb \approx -\Delta^{204}_{NFS}Pb$).

5.3.2 NFSE in crystals

The theoretical treatment of the NFSE requires quantum mechanics methods that can deal with relativistic quantum effects. Therefore, the Dirac equation-based methods are usually used. It is different from the Schrödinger equation-based methods for non-relativistic quantum chemistry calculations. The inner electrons (e.g., in s and p orbitals) of heavy elements run fast enough to produce large

relativistic effects. The outer electrons also have indirect relativistic effects. Both of them need the Dirac equation to deal with. The influences of relativistic effects about atomic structure are various, including the electron orbital contraction caused by the mass variation due to the high velocity and the coupling between electron spin and electron motion.

To date, a few computational methods for the study of quantum relativistic effects in connection with the NFSE are available. For example, the methods of Schauble (2007) and Yang and Liu (2015) take the quantum relativistic effects into account using the four-component Dirac equation in the DIRAC software package, the method of Abe et al. (2008a, b, 2010) uses a four-component relativistic atomic program package-GRASP2 K, and the method of Fujii et al. (2011a, b, 2013) uses a software provided by Tokyo University (Utchem). Recently, Nemoto et al. (2015) develop a two-component relativistic method (the finite-order Douglas–Kroll–Hess method with infinite-order spin–orbit interactions for the one-electron term and atomic-mean-field spin-same-orbit interaction for the two-electron term, i.e., IODKH-IOSO-MFSO) for the NFSE investigation. This method achieves almost equivalent accuracy but 30 times faster than the previous four-component method by the DIRAC software. The IODKH-IOSO-MFSO method has the potential to handle larger systems for the NFSE investigation in the future. However, it is still difficult to calculate the NFSE in crystals due to the relativistic effects of heavy elements. A few softwares, such as ABINIT and VASP, can calculate the properties of large molecules and crystals in the three-dimensional periodic boundary condition but must use pseudopotentials. More accurate methods for calculating the NFSE in very complex systems, such as crystals and melts, are yet to be developed. The methods for these systems need to consider the relativistic effects of heavy elements.

The above NFSE-calculations are only for the gaseous or small liquid species. To date, there is only one paper that reports the nuclear field shift effects in crystalline solids. Schauble (2013) estimated that the all-electron four-component Dirac–Hartree–Fock (DHF) method can be affordable only for systems with less than 20 atoms due to its computation intensity. Therefore, a density functional theory (DFT) based method is developed by Schauble (2013) to model the nuclear field shift effects in crystals. This new method uses the projector augmented wave method (DFT-PAW) with the three-dimensional periodic boundary condition for greater speed and compatibility (Schauble 2013).

Schauble (2013) compared the contact densities of a few species by the four-component relativistic Dirac–Hartree–Fock (DHF) method and by the DFT-PAW method (with the Perdew–Wang functional in the local density approximation and the Perdew, Burke, and Ernzerhof functional in the generalized gradient approximation methods), which are implemented in DIRAC and ABINIT software packages, respectively (Fig. 5). The calculated contact densities by DFT-PAW or DHF method for Hg, Sn– and Cd-bearing species are plotted into the Fig. 5a. The two sets of contact densities fall into a regression line with the slope close to 1.0, suggesting they are almost equivalent.

Equation (19) from King (1984) needs non-relativistic contact densities, which is not suitable for heavy elements with strong relativistic effects. Therefore, Schauble (2013) chose not to use Eq. (19) but to figure out a way that can indirectly obtain the energy shift (δT). He found that there is a good correlation between the contact densities [no matter obtained by DFT-PAW or by DHF) with the energy shifts calculated by the relativistic DHF and coupled-cluster (CCSD(T)] methods, where the nuclear charge distributions are varied due to different radii used in the Gaussian function for different isotopes (Fig. 5b–d). His results show that the difference in energies induced by isotope substitution calculated at CCSD (T) level is more strongly correlated with the contact densities of DFT-PAW than that of DHF level. The almost same correlation coefficients are obtained by the DFT-PAW models with PW and PBE functional (Schauble 2013). The results of Schauble (2013) in mercury crystals are shown in Fig. 4b.

5.4 Kinetic isotope fractionation of NFSE

When the forward reaction rate of a chemical reaction is much larger than the backward one, the kinetic isotope fractionation effect (KIE) often takes place. The classical transition state theory (TST) is proposed to deal with the elementary one-step reactions (Eyring 1935). According to the transition state theory, there must be an activated complex formed at the middle of the pathway from the reactant to the product (Fig. 6), where is at the highest point along the potential energy curve. The magnitude of the kinetic isotope effect can be calculated by using the theory proposed by Bigeleisen and Wolfsberg (1958), which suggests the KIE is just the equilibrium isotope fractionation between the transition state activated complex and the reactant. Their theory is based on high temperature approximation and neglects possible quantum (tunneling) effects. An empirical rule suggests that a molecule or a substance containing the light isotope will react faster than that containing heavy isotope, leading to the products to be enriched in light isotopes.

All the above experimental and theoretical studies of the NFSE are for equilibrium conditions. Fujii et al. (2009a) predicted if the NFSE-driven MIF in a kinetic system are related to the $\delta <r^2>$ trend, large MIFs can also be found in

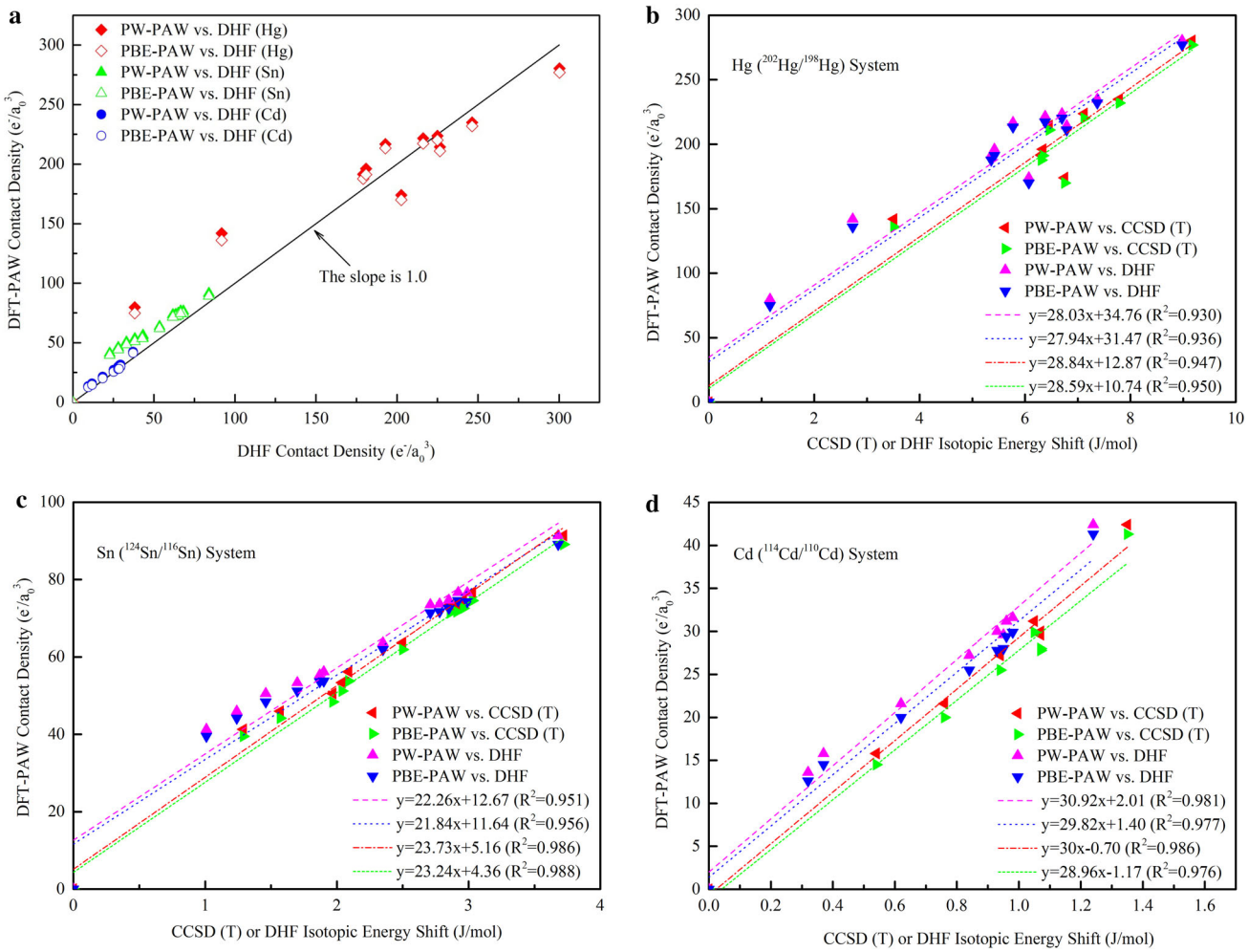

Fig. 5 Correlations of calculated contact densities with DFT-PAW methods and relativistic all-electron methods (Schauble 2013). **a** Contact densities calculated by DFT-PAW methods against Dirac–Hartree–Fock methods for Hg-, Sn-, and Cd-bearing molecules, respectively. The *black line* shows ideal 1:1 correlation. **b–d** Correlations of DFT-PAW contact densities with Dirac–Hartree–Fock (DHF) and coupled-cluster [CCSD(T)] isotopic energy shifts for $^{202}Hg/^{198}Hg$ relative to Hg^{2+}, $^{124}Sn/^{116}Sn$ relative to Sn^{4+}, and $^{114}Cd/^{110}Cd$ relative to Cd^{2+}, respectively

some reactions. Basu et al. (2014) conducted experiments of U(VI) reduction by bacterial isolates. They found that the reduced U [i.e., U(IV)] enriches heavier isotopes (^{238}U) in the kinetic reaction similar to the NFSE-driven isotope enrichments under the equilibrium condition which violates the generally accepted empirical rule. They attributed this anomalous isotope enrichment to the nuclear field shift effect. However, no theoretical calculation on the NFSE-driven KIE has been reported to date.

The electrons in s-orbital are important for the nuclear field shift effect which can cause larger electron density at the nucleus than p-, d-, f-orbitals. Heavier isotopes will prefer to be enriched in the species with fewer s electrons or more p, d and f electrons. Therefore, U(IV) enriches heavier isotopes (i.e., ^{238}U) relative to U(VI) in the reduction reaction from U(VI) to U(IV) no matter it is under equilibrium or kinetic conditions, because U(IV) and U(VI) are with the electron configuration as $[Rn]5f^2$ and [Rn], respectively. This phenomenon is against the general rule that heavier isotopes tend to enrich in the reactant rather than the product in a kinetic reaction. This anomalous enrichment phenomenon will also be for a few heavy elements in a kinetic system because of their smaller s-orbital or more p-, d-, f-orbital electrons, such as Hg^0 oxidized to Hg(II), Tl^0 oxidized to Tl(III), Pb^0 oxidized to Pb(IV), and U(IV) reduced to U(III).

6 Isotope geochronology

In natural systems, the abundance variations of natural radioisotopes record the geological time, and they are therefore effective tracers for geological processes. Isotopic geochronology, based on the accumulation of

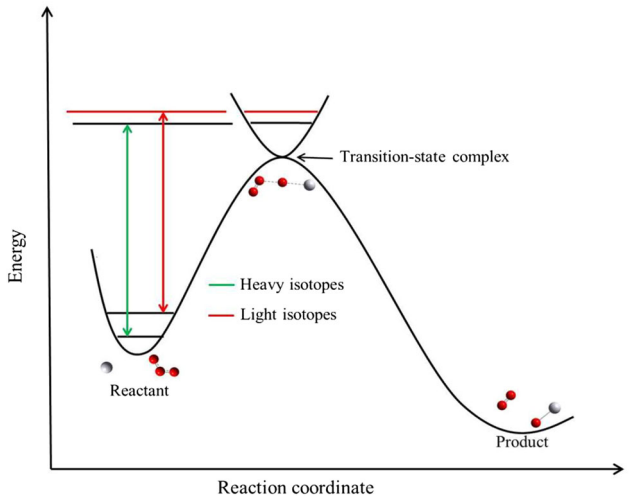

Fig. 6 The classical transition state theory (TST) and the way it deals with a kinetic reaction. There is an activated complex at the highest potential energy place alone the pathway from the reactant to the product (i.e., transition-state complex). The figure takes the kinetic reaction of Hg and O_3 as an example

radioisotopes with time, is a time keeper for closed geologic systems. Thus, radioisotope tracer can be used to study the genesis and evolution of the earth′s crust, mantle and other celestial bodies.

The base of radioisotope dating is the law of radioactive decay and it measures the isotope compositions of the parent and radiogenic daughter. It can be written as (White 2015)

$$D = D_0 + N(e^{\lambda t} - 1) \quad (25)$$

where N is the number of atoms of the parent and D is the total number of daughters, at time t; and D_0 is the original number of daughters. Taking the decay of ^{235}U to ^{207}Pb as an example, Eq. (25) becomes

$$^{207}Pb = {}^{207}Pb_0 + {}^{235}U(e^{\lambda}t - 1) \quad (26)$$

In practice, it generally measures the relative ratio of two isotopes, not the absolute abundance of one isotope in experiments. Therefore, Eq. (26) can be written as

$$\frac{^{207}Pb}{^{204}Pb} = \left(\frac{^{207}Pb}{^{204}Pb}\right)_0 + \frac{^{235}U}{^{204}Pb}(e^{\lambda t} - 1) \quad (27)$$

where ^{204}Pb is non-radiogenic isotope. Other decay systems can be written in similar expressions.

In the past, the accepted invariant value 137.88 of $^{238}U/^{235}U$ ratio was used for U–Pb and Pb–Pb dating. Nowadays, a few researches have verified that $^{238}U/^{235}U$ is not invariable (Stirling et al. 2007; Weyer et al. 2008; Hiess et al. 2012; Goldmann et al. 2015; Tissot and Dauphas 2015). Therefore, an age correction is required if the value of 137.88 ($^{238}U/^{235}U$ ratio) is used for dating. Goldmann et al. (2015) found the Pb–Pb ages they dated are 0.9 Ma younger than the age determined with previously assumed value 137.88 for $^{238}U/^{235}U$. Tissot and Dauphas (2015) proposed equations for the corrections on Pb–Pb and U–Pb ages, although these corrections are much smaller than the ages of the samples. The magnitude and direction of Pb–Pb and U–Pb age corrections are only related to a sample's age and $^{238}U/^{235}U$ ratio.

Many isotope dating methods are available for heavy elements that have large isotopic fractionations caused by the nuclear field shift effect, such as U-Th–Pb, Re–Os, Lu–Hf and Sm–Nd systematics. In these systems, the NFSE-driven fractionation will make the ratio of parent or daughter isotopes vary. It is unclear how the NFSE may affect the isotope age determination. This is an interesting topic for study using theoretical and experimental methods.

7 Summary

The nuclear field shift effect is an inherent property of heavy elements that induces large isotope fractionation. It is a mass-independent isotope fractionation driving force, which is originated from the difference in the ground-state electronic energies caused by differences in nuclear size and shape. The necessity of careful NFSE evaluation during the exploration of new heavy isotope systems is recognized by many researchers.

At different temperatures from 273 to 1000 K, the mass-dependent effect and the nuclear field shift effect scale as $1/T^2$ and $1/T$, respectively. At higher temperatures, the NFSE becomes more important than the MDE. With the rapid progress of experimental techniques and relativistic quantum chemistry, a better understanding of the nuclear field shift effect for heavy elements will emerge. However, there are still many details of the NFSE that need further investigation, such as the kinetic isotope effects (KIE), the NFSE in very large systems (e.g., solids, melts), and isotope geochronology.

Acknowledgments Y.L. are grateful for the funding support from the 973 Program (2014CB440904) and Chinese NSF projects (41225012, 41490635, 41530210).

References

Abe M, Suzuki T, Fujii Y, Hada M (2008a) An ab initio study based on a finite nucleus model for isotope fractionation in the U(III)–

U(IV) exchange reaction system. J Chem Phys 128:144309-1–144309-6
Abe M, Suzuki T, Fujii Y, Hada M, Hirao K (2008b) An ab initio molecular orbital study of the nuclear volume effects in uranium isotope fractionations. J Chem Phys 129:164309-1–164309-7
Abe M, Suzuki T, Fujii Y, Hada M, Hirao K (2010) Ligand effect on uranium isotope fractionations caused by nuclear volume effects: An ab initio relativistic molecular orbital study. J Chem Phys 133:044309-1–044309-5
Angeli I (2004) A consistent set of nuclear rms charge radii: properties of the radius surface R (N, Z). Atom Data Nucl Data Tables 87:185–206
Aufmuth P, Heilig K, Steudel A (1987) Changes in mean-square nuclear charge radii from optical isotope shifts. Atom Data Nucl Data Tables 37:455–490
Basu A, Sanford RA, Johnson TH, Lundstrom CC, LÖffler FE (2014) Uranium isotopic fractionation factors during U(VI) reduction by bacterial isolates. Geochim Cosmochim Acta 136:100–113
Bergquist BA, Blum JD (2007) Mass-dependent and –independent fractionation of Hg isotopes by photoreduction in aquatic systems. Science 318:417–419
Bigeleisen J (1996) Nuclear size and shape effects in chemical reaction. Isotope chemistry of the heavy elements. J Am Chem Soc 118:3676–3680
Bigeleisen J (1998) Second-order correction to the Bigeleisen–Mayer equation due to the nuclear field shift. Proc Natl Acad Sci USA 95:4809–4908
Bigeleisen J, Mayer MG (1947) Calculation of equilibrium constants for isotopic exchange reactions. J Chem Phys 15:261–267
Bigeleisen J, Wolfsberg M (1958) Theoretical and experimental aspects of isotope effects in chemical kinetics. Adv Chem Phys 1:15–76
Cao XB, Liu Y (2011) Equilibrium mass-dependent fractionation relationships for triple oxygen isotopes. Geochim Cosmochim Acta 75:7435–7445
Chen JR, Nomura M, Fujii Y, Kawakami F, Okamoto M (1992) Gadolinium isotope separation by cation exchange chromatography. J Nucl Sci Technol 29:1086–1092
Chen JB, Hintelmann H, Feng XB, Dimock B (2012) Unusual fractionation of both odd and even mercury isotopes in precipitation from Peterborough, ON, Canada. Geochim Cosmochim Acta 90:33–46
Dujardin T, Lonchampt G (1992) In: Fujii Y, Ishida T, Takeuchi K (eds), Uranium enrichment, Proceedings of international symposium on isotope separation and chemical exchange. Bull Res Lab Nucl React, Tokyo Institute of Technology, Tokyo
Estrade N, Carignan J, Sonke JE, Donard OFX (2009) Mercury isotope fractionation during liquid-vapor evaporation experiments. Geochim Cosmochim Acta 73:2693–2711
Eyring H (1935) The activated complex in chemical reactions. J Chem Phys 3:107–115
Fricke G, Heilig K (2004) 92-U Uranium. Landolt-Boernstein. Numerical data and functional relationships in science and technology. Group I: element particles, nuclei and atoms. Springer, Heidelberg vol 20, pp 1–5. Nuclear Charge Radii
Fujii Y, Nomura M, Onitsuka H, Takeda K (1989a) Anomalous isotope fractionation in uranium enrichment process. J Nucl Sci Technol 26:1061–1064
Fujii Y, Nomura M, Okamoto M, Onitsuka H, Kawakami F, Takeda K (1989b) An anomalous isotope effect of ^{235}U in U(IV)-U(VI) chemical exchange. Z Naturforsch A 44:395–398
Fujii T, Inagawa J, Nishizawa K (1998a) Influences of nuclear mass, size, shape and spin on chemical isotope effect of titanium. Ber Burtsenges Phys Chem 102:1880–1885
Fujii T, Yamamoto T, Inagawa J, Watanabe K, Nishizawa K (1998b) Influences of nuclear size and shape and nuclear spin on chemical isotope effect of zirconium-crown complex. Ber Burtsenges Phys Chem 102:663–669
Fujii T, Kawashiro F, Yamamoto T, Nomura M, Nishizawa K (1999a) Contribution of nuclear size and shape to chemical enrichment of iron isotopes. Solv Extr Ion Exch 17:177–190
Fujii T, Yamamoto T, Inagawa J, Gunji K, Watanabe K, Nishizawa K (1999b) Nuclear size and shape effect in chemical isotope effect of gadolinium using dicyclohexano-18-crown-6. Solv Extr Ion Exch 17:1219–1229
Fujii T, Yamatomo T, Inagawaa J, Gunji K, Watanabe K, Nishizawa K (2000) Nuclear size and shape effects in chemical isotope enrichment of neodymium using a crown ether. SolvExtr Ion Exch 18:1155–1166
Fujii T, Suzuki D, Gunji K, Watanabe K, Moriyama H, Nishizawa K (2002) Nuclear field shift effect in the isotope exchange reaction of chromium(III) using a crown ether. J Phys Chem A 106:6911–6914
Fujii T, Moynier F, Albarede F (2006a) Nuclear field vs. nucleosynthetic effects as cause of isotopic anomalies in the early Solar System. Earth Planet Sci Lett 247:1–9
Fujii T, Moynier F, Telouk P, Albarede F (2006b) Mass-independent isotope fractionation of molybdenum and ruthenium and the origin of isotopic anomalies in Murchison. Astrophys J 647:1506–1516
Fujii Y, Higuchi N, Haruno Y, Nomura M, Suzuki T (2006c) Temperature dependence of isotope effects in uranium chemical exchange reactions. J Nucl Sci Technol 43:400–406
Fujii T, Suzuki D, Yamana H (2008) Nuclear field shift effect of chromium(III) in repeated extraction using a crown ether. Solv Extr Ion Exch 26:100–112
Fujii T, Moynier F, Albarede F (2009a) The nuclear field shift effect in chemical exchange reactions. Chem Geol 267:139–156
Fujii T, Moynier F, Telouk P, Albarede F (2009b) Nuclear field shift effect in the isotope exchange reaction of cadmium using a crown ether. Chem Geol 267:157–163
Fujii T, Moynier F, Uehara A, Abe M, Yin QZ, Nagai T, Yamana H (2009c) Mass-dependent and mass-independent isotope effects of zinc in a redox reaction. J Phys Chem A 113:12225–12232
Fujii T, Moynier F, Telouk P, Abe M (2010) Experimental and Theoretical Investigation of Isotope Fractionation of Zinc between Aqua, Chloro, and Macrocyclic Complexes. J Phy Chem A 114:2543–2552
Fujii T, Moynier F, Agranier A, Ponzevera E, Abe M (2011a) Nuclear field shift effect of lead in ligand exchange reaction using a crown ether. Proc Radiochim Acta 1:387–392
Fujii T, Moynier F, Dauphas N, Abe M (2011b) Theoretical and experimental investigation of nickel isotopic fractionation in species relevant to modern and ancient oceans. Geochim Cosmochim Acta 75:469–482
Fujii T, Moynier F, Agranier A, Ponzevera E, Abe M, Uehara A, Yamana H (2013) Nuclear field shift effect in isotope fractionation of thallium. J Radioanal Nucl Chem 296:261–265
Ghosh S, Xu XF, Humayun M, Odom L (2008) Mass-independent fractionation of mercury isotopes in the environment. Geochem Geophy Geosy 9:Q03004. doi:10.1029/2007GC001827
Ghosh S, Schauble EA, Couloume GL, Blum JD, Bergquist BA (2013) Estimation of nuclear volume dependent fractionation of mercury isotopes in equilibrium liquid-vapor evaporation experiments. Chem Geol 336:5–12
Goldmann A, Brennecka G, Noordmann J, Weyer S, Wadhwa M (2015) The uranium isotopic composition of the Earth and the Solar System. Geochim Cosmochim Acta 148:145–158
Gratz LE, Keeler GJ, Blum JD, Sherman LS (2010) Isotopic composition and fractionation of mercury in great lakes precipitation and ambient air. Environ Sci Technol 44:7764–7770

Hahn AA, Miller JP, Powers RJ, Zehnder A, Rushton AM, Welsh RE, Kunselman AR, Roberson P (1979) Experimental-study of muonic X-ray transitions in mercury isotopes. Nucl Phys 314:361–386

Heilig K, Steudel A (1978) In: Hanel W, Kleinpoppen H (eds) Progress in atomic spectroscopy, part A. Plenum Press, New York, pp 263–328

Hiess J, Condon DJ, McLean N, Noble SR (2012) $^{238}U/^{235}U$ systematics in terrestrial uranium-bearing minerals. Science 335:1610–1614

King WH (1984) Isotope shifts in atomic spectra. Plenum Press, New York

Kleinman LI, Wolfsberg M (1973) Corrections to the Born-Oppenheimer approximation and electronic effects on isotopic exchange equilibria. Chem Phys 59:2043–2053

Kleinman LI, Wolfsberg M (1974) Corrections to the Born-Oppenheimer approximation and electronic effects on isotopic exchange equilibria. 2. Chem Phys 60:4740–4748

Lerat JM, Lorrain C (1985) Solvent extraction and ion exchange in the nuclear fuel cycle. Soc Chem Ind, Ellis Horwood Ltd., London

Miller MF (2002) Isotopic fractionation and the quantification of O-17 anomalies in the oxygen three-isotope system: an appraisal and geochemical significance. Geochim Cosmochim Acta 66:1881–1889

Moynier F, Fujii T, Albarède F et al (2009a) Nuclear field shift effect as a possible cause of Te isotopic anomalies in the early solar system-an alternative explanation of Fehr et al. 2006–2009. Meteorit Planet Sci 44:1735–1742

Moynier F, Fujii T, Telouk P (2009b) Mass-independent isotope fractionation of tin in chemical exchange reaction using a crown ether. Anal Chim Acta 632:234–239

Moynier F, Fujii T, Brennecka GA, Nielsen SG (2013) Nuclear field shift in natural environments. C R Geoscience 345:150–159

Nemoto K, Abe M, Seino J, Hada M (2015) An ab intio study of nuclear volume effects for isotope fractionations using two-component relativistic methods. J Comput Chem 36:816–820

Nishizawa K, Nakamura K, Yamamoto T, Masuda T (1993) Zinc isotope effects in complex-formation with a crown–ether. Solv Extr Ion Exch 11:389–394

Nishizawa K, Nakamura K, Yamamoto T, Masuda T (1994) Separation of strontium and barium isotopes using a crown–ether. Different behaviors of odd mass and even mass isotopes. Solv Extr Ion Exch 12:1073–1084

Nishizawa K, Satoyama T, Miki T, Yamamoto T (1995) Strontium isotope effect in liquid-liquid extraction of strontium chloride using a crown ether. J Nucl Sci Technol 32:1230–1235

Nishizawa K, Maeda Y, Kawashiro F, Fujii T, Yamamoto T (1998) Contributions of nuclear size and shape, nuclear spin to enrichment factors of zinc isotopes in a chemical exchange reaction by a cryptand. Separ Sci Technol 33:2101–2112

Nomura M, Higuchi N, Fujii Y (1996) Mass dependence of uranium isotope effects in the U(IV) − U(VI) exchange reaction. J Am Chem Soc 118:9127–9130

Schauble EA (2007) Role of nuclear volume in driving equilibrium stable isotope fractionation of mercury, thallium, and other very heavy elements. Geochim Cosmochim Acta 71:2170–2189

Schauble EA (2013) Modeling nuclear volume isotope effects in crystals. Proc Natl Acad Sci USA 110:17714–17719

Shibahara Y, Nishizawa K, Yasaka Y, Fujii T (2002a) Strontium isotope effect in dmso-water system by liquid chromatography using a cryptand polymer. Solv Extr Ion Exch 20:67–79

Shibahara Y, Takaishi H, Nishizawa K, Fujii T (2002b) Strontium isotope effects in ligand exchange reaction. J Nucl Sci Technol 39:451–456

Stacey DN (1966) Isotope shifts and nuclear charge distributions. Rep Prog Phys 29:171–215

Stirling C, Andersen MB, Potter EK, Halliday AN (2007) Low-temperature isotopic fractionation of uranium. Earth Planet Sci Lett 264:208–225

Tissot FLH, Dauphas N (2015) Uranium isotopic compositions of the crust and ocean: Age corrections, U budget and global extent of modern anoxia. Geochim Cosmochim Acta 167:113–143

Urey HC (1947) The thermodynamic properties of isotopic substances. J Chem Soc (London) 85:562–581

Wang XL, Johnson TM, Lundstrom CC (2015) Low temperature equilibrium isotope fractionation and isotope exchange kinetics between U(IV) and U(VI). Geochim Cosmochim Acta 158:262–275

Weyer S, Anbar A, Gerdes A, Gordon G, Algeo T, Boyle E (2008) Natural fractionation of $^{238}U/^{235}U$. Geochim Cosmochim Acta 72:345–359

White WM (2015) Isotope geochemistry. Wiley, Chichester

Wiederhold JG, Cramer CJ, Daniel K, Infante I, Bourdon B, Kretzschmar R (2010) Equilibrium mercury isotope fractionation between dissolved Hg(II) species and thiol-bound Hg. Environ Sci Technol 44:4191–4197

Yang S, Liu Y (2015) Nuclear volume effects in equilibrium stable isotope fractionations of mercury, thallium and lead. Sci Rep 5:12626. doi:10.1038/srep12626

Young ED, Galy A, Nagahara H (2002) Kinetic and equilibrium mass-dependent isotope fractionation laws in nature and their geochemical and cosmochemical significance. Geochim Cosmochim Acta 66:1095–1104

Zheng W, Hintelmann H (2009) Mercury isotope fractionation during photoreduction in natural water is controlled by its Hg/DOC ratio. Geochim Cosmochim Acta 73:6704–6715

Zheng W, Hintelmann H (2010a) Nuclear field shift effect in isotope fractionation of mercury during abiotic reduction in the absence of light. J Phys Chem A 114:4238–4245

Zheng W, Hintelmann H (2010b) Isotope fractionation of mercury during its photochemical reduction by low-molecular-weight organic compounds. J Phys Chem A 114:4246–4253